

words than digits (in this case) also plays a role in reducing the overall accuracy of word recognition relative to digit recognition.

IV. CONCLUSION

This study presented an HMM approach to dysarthric speech recognition using three types of feature vectors in order to investigate the robustness and accuracy of the various models, wherein a ten-state ergodic model, with MFCC vectors extracted using 15 ms frames, was found to be more accurate than others studied. Data from three cerebral palsy individuals were used to test the models. However, the results may also be equally applicable to dysarthric individuals other than those with cerebral palsy, say, people with neurogenic communication disorders. This could be further expanded to accommodate a larger vocabulary and, thus, is part of an effort to develop an artificially intelligent communication/control tool, either in standalone mode or in conjunction with other methods like eye tracking, etc., for speech and motor impaired individuals.

REFERENCES

- [1] X. Menendez-Padial *et al.*, "The nemours database of dysarthric speech," in *Proc. 4th Int. Conf. Spoken Language Process.*, Philadelphia, PA, Oct. 1996, pp. 1962–1965.
- [2] C. J. Gold, *Cerebral Palsy—John Coopersmith Gold*. Berkeley Heights, NJ: Enslow, 2001.
- [3] J. M. Noyes and C. R. Frankish, "Speech recognition technology for individuals with disabilities," *Augmentative Alternative Commun.*, vol. 8, pp. 297–303, 1992.
- [4] L. R. Rabiner, "A tutorial on hidden Markov models and selected applications in speech recognition," *Proc. IEEE*, vol. 77, no. 2, pp. 257–286, Feb. 1989.
- [5] J. R. Deller Jr, D. Hsu, and L. J. Ferrier, "On the use of hidden Markov modeling for recognition of dysarthric speech," *Comput. Methods Programs Biomed.*, vol. 35, pp. 125–139, 1991.
- [6] F. Chen and A. Kostov, "Optimization of dysarthric speech recognition," in *IEEE EMBS Conf.*, vol. 4, Chicago, IL, Oct. 30–Nov. 2 1997, pp. 1436–1439.
- [7] C. Bickley and N. Talbot, "TIDE-ENABLE: Engineering design using language and speech," in *Proc. Resna Annu. Conf.*, Orlando, FL, Jun. 2000, pp. 76–78.
- [8] G. Jayaram and K. Abdelhamid, "Experiments in dysarthric speech recognition using artificial neural networks," *J. Rehabil. Res. Devel.*, vol. 32, no. 2, pp. 162–169, 1995.
- [9] M. Parker *et al.* (2003) STARDUST Project-Speech Recognition for People With Severe Dysarthria. Dept. Health, Univ. Sheffield, U.K. [Online]. Available: <http://www.dcs.shef.ac.uk/~pdg/stardust>
- [10] P. Green, J. Carmichael, A. Hatzis, P. Enderby, M. Hawley, and M. Parker, "Automatic speech recognition with sparse training data for dysarthric speakers," *Eurospeech*, pp. 1189–1192, 2003.
- [11] A. Hatzis, P. Green, J. Carmichael, S. Cunningham, R. Palmer, M. Parker, and P. O'Neill, "An integrated toolkit deploying speech technology for computer based speech training with application to dysarthric speakers," *Eurospeech*, pp. 2213–2216, 2003.
- [12] B. Mak, Y. C. Tam, and Q. Li, "Discriminative auditory-based features for robust speech recognition," *IEEE Trans. Speech Audio Process.*, vol. 12, no. 1, pp. 27–36, Jan. 2004.
- [13] W. J. Tompkins and J. G. Webster, *Design of Microcomputer Based Medical Instrumentation*. Englewood Cliffs, NJ: Prentice Hall, 1981.
- [14] F. Jelinek, *Statistical Methods for Speech Recognition (Language, Speech, and Communication: A Bradford Book)*. Cambridge, MA: MIT Press, Jan. 1998.
- [15] T. L. Pao, Y. T. Chen, J. H. Yeh, and J. J. Lu. Detecting emotions in Mandarin speech. presented at Proc. Rocling XVI. [Online]. Available: <http://www.aclclp.org.tw/rocling/2004/M38.pdf>

A Low-Noise Preamplifier for Nerve Cuff Electrodes

Mesut Sahin

Abstract—A single-stage, low-noise preamplifier is designed using the concept of noise matching for recordings of neural signal with cuff electrodes. The signal-to-noise ratio is approximately 1.6 times higher than that of a low-noise integrated amplifier (AMP-01) for a cuff impedance of 1.5 k Ω . The bandwidth is 230 Hz–8.25 kHz ($R_s=2$ k Ω), and the common-mode-rejection-ratio is 91.2 dB at 1 kHz.

Index Terms—Nerve electrodes, neural recording, noise reduction.

I. INTRODUCTION

The neural signal amplitudes are in the order of a few microvolts when the activity of a large peripheral nerve is recorded with a cuff electrode [1]. The electroneurogram (ENG) signals are usually contaminated by electromyogram (EMG) activity from the surrounding muscles, the thermal noise generated within the source resistance, i.e., the resistive component of the nerve/electrode lumped impedance, and the electronic noise generated primarily at the first stage of the neural amplifier.

The EMG and ENG signal spectra overlap only partially and, therefore, one can use linear filtering methods to suppress the EMG component by sacrificing some ENG signal power. However, the linear filtering approaches are not effective to reduce the thermal and electronic noise components since they encompass the entire ENG spectrum. The thermal noise of the source and electronic noise together constitute the baseline noise in neural recordings and present a challenging problem especially when the ENG components are only in the order of one or two microvolts. The thermal noise of the source can only be lowered by optimizing the neural electrode geometry [2] and the size of the interface with the neural tissue, which are determined by the space available at the implantation site. The concept of source noise needs to be dealt with elsewhere in the context of electrode geometry.

The electronic noise contribution of the preamplifier, which is the subject of this report, is negligible for source impedance values larger than 10 k Ω . That is, the thermal noise of the source is already so large that even a marginal amplifier can amplify the signals without deteriorating the signal-to-noise ratio (SNR). On the other hand, the electronic noise is significant even with very-low-noise integrated amplifiers when the source is as small as 1 k Ω , and it becomes the main factor deteriorating the SNR.

This paper describes a transformer preamplifier design that is optimized for peripheral nerve recordings with cuff electrodes and compares it with an integrated amplifier [AMP-01 (Analog Devices, Inc., Norwood, MA)], which is one of the best bipolar input amplifiers to be used with small sources. The use of transformers for noise matching is a well-known concept in electrical engineering [3], [4]. Transformers were favored as the first stage of neural amplifiers both for matching the source to the input characteristics of the amplifier and for their filtering property at low frequencies which resulted in reduction of EMG and direct current (dc) coupling artifacts [5]. In another report, an audio transformer was used as the first stage of an ENG amplifier design for 1) passively amplifying the signals and 2) minimizing the interference from the power lines [6]. However, the concept of noise matching was

Manuscript received February 7, 2005; revised April 27, 2005; accepted June 20, 2005.

The author is with the Biomedical Engineering Department, Louisiana Technical University, Ruston, LA 71272 USA (e-mail: sahin@coes.latech.edu).
Digital Object Identifier 10.1109/TNSRE.2005.856073

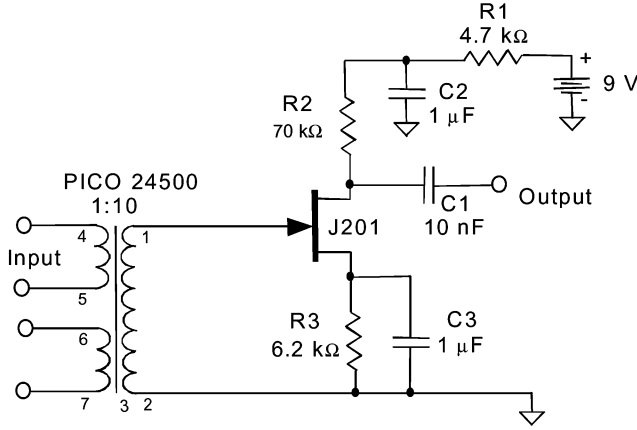


Fig. 1. Low-noise preamplifier design for neural recording. Transformer is used to match the noise characteristics of the source to that of the FET input. Drain current, which is the total current drawn from the power supply, is $97 \mu\text{A}$ with a 9-V battery.

not one of the design criteria considered in these reports to minimize the electronic noise, with an exception of an abstract [7]. The main objective in this report is to provide a single-stage (few components), practical, low-noise preamplifier design that is optimized for cuff electrodes with small impedances. Practical considerations for the transformer design are discussed for those who would like to build their own transformer to match different sources. Because of its low current consumption, this amplifier design may also find use in implantable devices wherever the space taken by a small transformer is acceptable.

II. CIRCUIT DESIGN

A. FET Amplifier

A low-noise field-effect transistor (FET) (J201, Siliconix) is chosen for the design of the amplifier with the following characteristics: Equivalent input voltage noise: $\bar{e}_n = 6 \text{ nV}/\sqrt{\text{Hz}}$ ($V_{DG} = 10 \text{ V}$, $I_D = 0.1 \text{ mA}$, $f = 1 \text{ kHz}$), equivalent input current noise: $\bar{i}_n = 0.6 \text{ fA}/\sqrt{\text{Hz}}$ ($V_{DG} = 10 \text{ V}$, $I_D = 0.1 \text{ mA}$, $f = 1 \text{ kHz}$), and common-source forward transconductance (g_{fs}) = 0.5 mS (at $f = 1 \text{ kHz}$). In the proposed circuit design (Fig. 1), the gate is kept at ground potential through the secondary coil of the noise-matching transformer (PICO 24500, microphone audio input transformer, Pico Electronics Inc., NY), and the gate-source junction is biased near the pinch-off point with a source resistor (R3). The corner frequency of the highpass filter that consists of R3 and C3 is set around $f = 25 \text{ Hz}$. The gain of the FET stage is maximized by adjusting the drain resistor R2. The maximum voltage gain is obtained when the drain current is approximately $97 \mu\text{A}$ and $R2 = 70 \text{ k}\Omega$. The capacitor C1 serves as a coupling capacitor to the next stage. The capacitor C2 and R1 are used to suppress the noise generated within the power supply (in case a voltage regulator is used instead of a 9-V battery) before it is fed back to the gate through the internal gate-drain capacitor of the FET.

B. Noise Matching Transformer

The intrinsic noise of an amplifier, which is mostly due to the thermal noise generated at its input stage, can be modeled with equivalent voltage (\bar{e}_n) and current (\bar{i}_n) sources (Fig. 2). Matching the internal resistance (R_S) of the signal source (e_S) to the ratio of \bar{e}_n over \bar{i}_n using a transformer is termed as “noise matching,” and it maximizes the SNR at the output [3]. Note that matching R_S to the input impedance of the amplifier, which is power matching, does not necessarily increase the SNR. The optimal source resistance and the

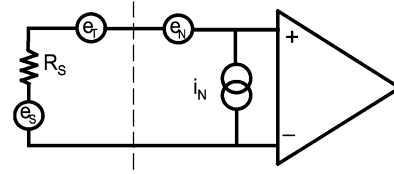


Fig. 2. Equivalent circuit model of a practical signal source and an amplifier with the input noise characteristics. e_N : equivalent input voltage noise. i_N : equivalent input current noise. e_S : signal source. R_S : source resistor (noiseless). e_T : thermal noise of the source resistor.

turn ratio for the matching transformer are given by the following equations:

$$R_{SO} = \frac{\bar{e}_N}{\bar{i}_N} \quad (1)$$

$$n = \sqrt{\frac{R_{SO}}{R_S}} \quad (2)$$

where R_{SO} is the optimum input resistance to the amplifier and R_S is the actual source resistance.

Since the noise sources are uncorrelated, the total input voltage noise per $\sqrt{\text{Hz}}$ can be expressed as a summation of the thermal noise (\bar{e}_T) due to the source resistance and the voltage and current noise of the amplifier’s input stage

$$\bar{e}_{Ni} = \sqrt{\bar{e}_T^2 + \bar{e}_n^2 + \bar{i}_n^2 \times R_S^2}. \quad (3)$$

The equivalent input voltage and current noise values for J201, given by the manufacturer, are $6 \text{ nV}/\sqrt{\text{Hz}}$ and $0.6 \text{ fA}/\sqrt{\text{Hz}}$, respectively, for the frequency band of interest. Thus, the optimum source resistance that matches the input noise characteristics of this transistor is $10 \text{ M}\Omega$ [see (1)]. The cuff electrodes designed for recording the neural activity from peripheral nerves have impedances in the range of $1\text{--}10 \text{ k}\Omega$ depending on the size of the electrode and the metal contacts. If we assume a low value for the cuff ($1.5 \text{ k}\Omega$), the turn ratio of the input transformer that matches the source to the input noise characteristics of J201 and, thereby, maximizes the output SNR, can be found as $n = 82$ using the (1) and (2). However, such a high turn ratio for the transformer imposes a limit on the cutoff frequency of the circuit, as discussed below.

C. Practical Considerations on the Transformer Design

In the proposed design, the impedance presented to the FET gate by the secondary coil of the transformer is the source resistor times the square of the transformer turn ratio ($R_S n^2$). This impedance quickly gets into the mega ohm range with increasing values of n for a given R_S . The secondary impedance and the input capacitance of the FET form a low-pass filter that dictates the higher cutoff frequency of the circuit. Therefore, a trade-off exists between the turn ratio of the transformer and the bandwidth of the circuit (R_S is fixed). The larger the turn ratio, the lower the cutoff frequency. Apart from this tradeoff, a low value for the gate capacitance is desirable since this would increase the bandwidth independently without reducing the turn ratio.

Another design criteria is the impedance presented to the signal source by the transformer. The primary coil magnetizing impedance should be made as large as possible to prevent shunting of the signal source. This implies that the transformer core size needs to be increased. Thus, the transformer cannot be made smaller than a certain size in order to keep the shunting effect of the source negligible.

Considering the criteria above, a commercially available nickel alloy transformer (24500, PICO Inc., 19 mm diameter, 18 mm height) was selected as the optimal choice balancing these trade-offs. The magnetizing coil impedance ($10 \text{ k}\Omega$) is six–seven times larger than the

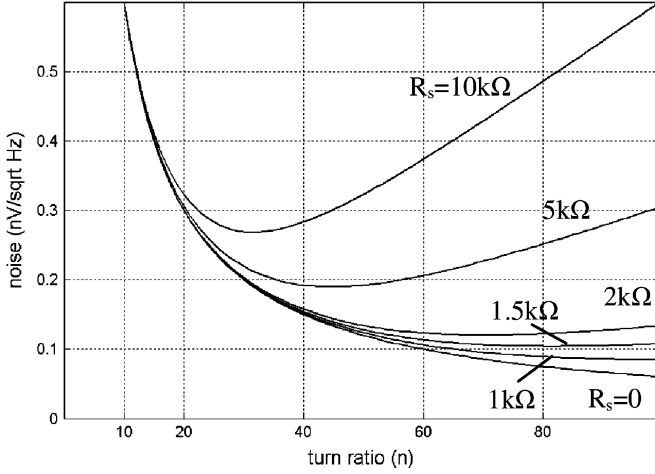


Fig. 3. Theoretical input noise of the transformer-coupled amplifier as the turn ratio is varied from 1 to 100. Several values of the (actual) source resistance (R_s) are considered. Thermal noise (e_T) due to the source itself is not included into the plots to emphasize the electronic noise component.

source impedance considered (1.5 k Ω) and, thereby, not shunting the source significantly at mid-frequencies. The turn ratio is 10 instead of the optimal value of 82. This is about the highest practically achievable turn ratio (as determined by a search on commercially available transformers) if the frequency bandwidth should extend up to 8 kHz for $R_s = 2$ k Ω . This value of n can sufficiently reduce the electronic noise of J201 and make it virtually zero compared to the thermal noise of a few kilohm source. The electronic noise of the amplifier is plotted in Fig. 3 for several values of the source resistance and the transformer turn ratio ranging from 1 to 100. Equation (3) was used to generate the plots except that the thermal noise of the source resistance (e_T) was not included to illustrate the contribution of the amplifier alone. The plots show that the optimum turn ratio that minimizes the noise decreases as a function of the actual source resistance (R_s) as predicted by (2). The curve for $R_s = 1.5$ k Ω indicates that the electronic noise contribution of the amplifier increases from about 0.1–0.6 nV/ $\sqrt{\text{Hz}}$ when the turn ratio decreases from its optimal value of 82 down to 10. Compared to the thermal noise of a 1500 Ω resistor (4.925 nV/ $\sqrt{\text{Hz}}$ at 20 $^\circ\text{C}$), 0.6 nV/ $\sqrt{\text{Hz}}$ is still relatively small and its contribution to the total input noise is only 0.7% (3). If the turn ratio is further decreased, the benefit on the noise reduction quickly diminishes as the plots sharply increase to the left of Fig. 3.

The thermal noise generated in the primary coil resistance of the selected transformer should be negligible compared to that of the source resistance. When two uncorrelated random noise sources are added, the variation of the sum is given by

$$\sigma^2 = \sigma_x^2 + \sigma_y^2. \quad (4)$$

For a fixed bandwidth and temperature, the thermal noise is proportional to the square root of the resistance as given by the Boltzmann equation

$$(\overline{e_T}) = \sqrt{4kTBR} \quad (5)$$

where k is the Boltzmann's constant (1.38×10^{-23} J/K), T is temperature in Kelvin, B is the frequency bandwidth, and R is the resistance in which the thermal noise is generated. The primary coil resistance for PICO 24500 (R_{coil}) is about 50 Ω . The noise contribution of this R_{coil} to the thermal noise of a source of 1.5 k Ω is only 1.7% (4) when the noise standard deviation is calculated with (5) for each resistor.

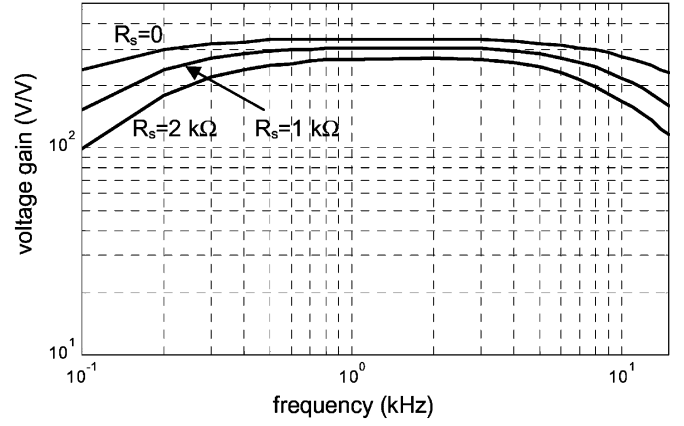


Fig. 4. Voltage gain versus frequency plot of the amplifier shown in Fig. 1 for three different values of the source resistor ($R_s = 0, 1, \text{ and } 2$ k Ω).

III. GAIN, CMRR, AND INPUT IMPEDANCE MEASUREMENTS

The amplifier gain was measured between 100 Hz and 15 kHz with a resistor in series to the input ($R_s = 0, 1, \text{ and } 2$ k Ω metal film resistors) simulating the neural electrode impedance (Fig. 4). The overall gain and the bandwidth decreased with increasing source resistance. The gain was 333 305, and 274 for $R_s = 0, 1, \text{ and } 2$ k Ω , respectively, at 2 kHz. The low and high cutoff frequencies were 90 Hz–14 kHz, 160 Hz–10 kHz, and 230 Hz–8.25 kHz for the same values of the source resistor. The common-mode-rejection-ratio (CMRR) was measured at 100 Hz, 1 kHz, and 10 kHz as 111.3 dB (a ratio of 368 000), 91.2 dB (36 486), and 69.7 dB (3038), respectively.

The input impedance (using only one of the primary coils of the transformer) was about 10 k Ω at 2 kHz and flat between 500 Hz and 10 kHz. The input impedance dropped by -3 dB at 160 Hz from that of its value at 2 kHz.

IV. NOISE MEASUREMENTS

To plot the noise spectra, the signal source was removed and the input was terminated with R_s only. The output was further amplified (Gain = 10 000, Nanovolt Amplifier, Model 103A, Keithley Inc.), filtered to prevent aliasing (BW = 1 Hz–30 kHz), and acquired into a computer at a sampling rate of 200 000 samples/s using LabVIEW software and a data acquisition board (PCI-6071E, National Instruments). Fourier coefficients were calculated using MATLAB for a 20-s-long acquisition for each value of R_s . Adjacent Fourier coefficients were averaged in groups of 20 so that each coefficient represented the voltage noise per $\sqrt{\text{Hz}}$. The noise measurements were divided by the overall gain of the system at each frequency to find the input referred voltage noise and its magnitude is plotted in Fig. 5. The theoretical thermal noise levels generated in 1 and 2 k Ω resistors at 20 $^\circ\text{C}$ [see (5)] are also shown in the plots for comparison. The total input-referred noise measured, which includes both the noise of the source resistor and the amplifier, is slightly over that of the thermal noise for the source resistor alone. This indicates that the noise contribution from the amplifier is relatively much smaller than the source noise *per se*. The rise toward the lower end of the spectrum is possibly due to the flicker noise of the input current that is intrinsic to the FET. Because it is a current noise, it does not affect the spectrum for $R_s = 0$. The SNR of the source should approximately be preserved at the amplifier's output since the electronic noise is very small compared to that of the source.

Similar noise measurements (Fig. 6) were conducted for an amplifier built with AMP-01 (Analog Devices, Inc.) following the connection diagram suggested by the manufacturer for a gain of 1000. The input noise is larger than that of a 1-k Ω resistor even when the input is short

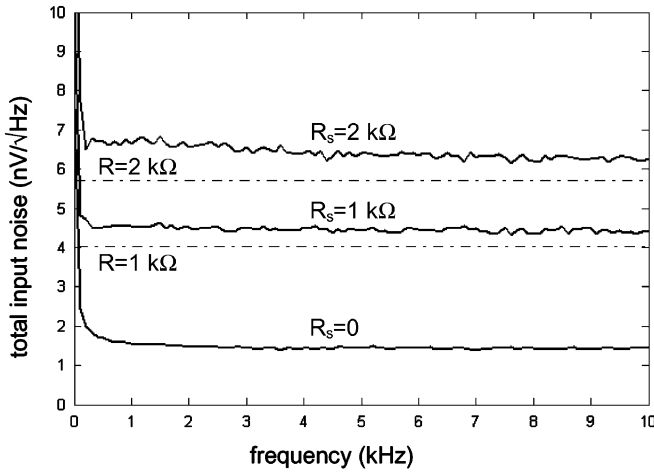


Fig. 5. Total input noise of the amplifier shown in Fig. 1 for three values of the source resistance ($R_s = 0, 1, \text{ and } 2 \text{ k}\Omega$). Input noise is obtained by dividing the measured output noise by the gain values plotted in Fig. 4 at each frequency. Theoretical thermal noise level generated within 1 and 2 $\text{k}\Omega$ resistors are also shown for comparison (dash lines at 4.02 and 5.7 $\text{nV}/\sqrt{\text{Hz}}$).

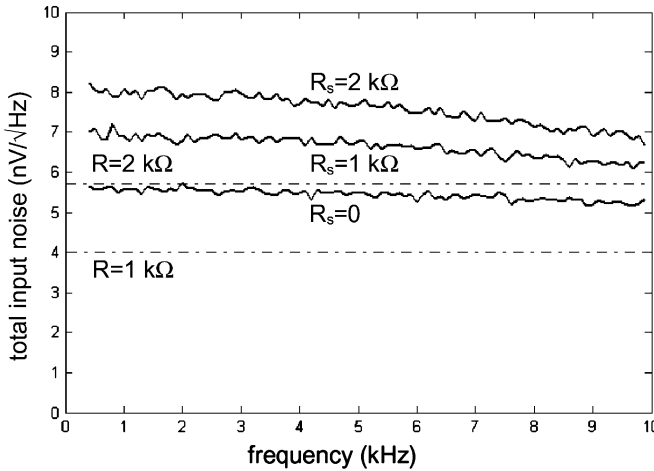


Fig. 6. Total input noise of an amplifier designed with AMP-01 is shown for the same values of the source resistance as in Fig. 5. Theoretical thermal noise generated within 1 and 2 $\text{k}\Omega$ resistors are also shown for comparison (dash lines).

circuit ($R_s = 0$). Further comparison of Figs. 5 and 6 reveals that the proposed amplifier has less noise for all three input termination conditions while the most drastic difference occurs when the input is short circuit ($R_s = 0$).

V. SALINE TANK EXPERIMENTS

The total input noise of the proposed and the AMP-01 based amplifiers were measured experimentally in a saline tank setup as depicted in Fig. 7. The sinusoidal signal generator simulated a neural signal source, which induced a voltage across a cylindrical nerve cuff electrode placed in the tank. The electrode was fabricated using silicone substrate and platinum contacts. The amplifiers were connected, one at a time, to the platinum contacts on each end of the cuff electrode differentially. The bipolar impedance of the electrode was about 1.5 $\text{k}\Omega$ near the lower end of the spectrum (at 1 kHz) and decreased gradually down to 1.15 $\text{k}\Omega$ at 10 kHz.

Several cycles of the sinusoidal waveform, recorded with each one of the amplifiers, are shown in Fig. 8 for comparison. The signal source

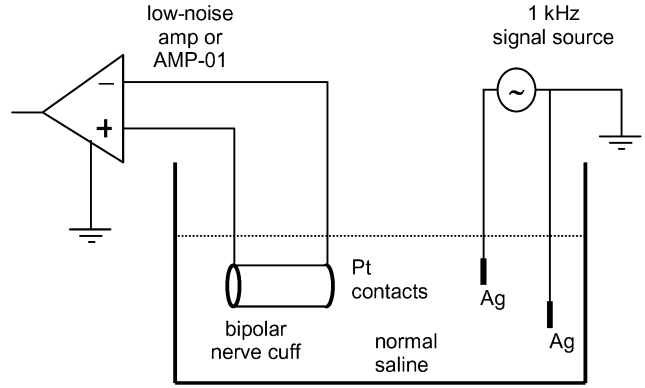


Fig. 7. Experimental setup used to measure the SNR of the proposed and the AMP-01 amplifiers for comparison. A sinusoidal signal source at 1 kHz generates a voltage field through the silver electrodes placed in the tank. Signal is recorded with a bipolar nerve cuff electrode simulating an implant.

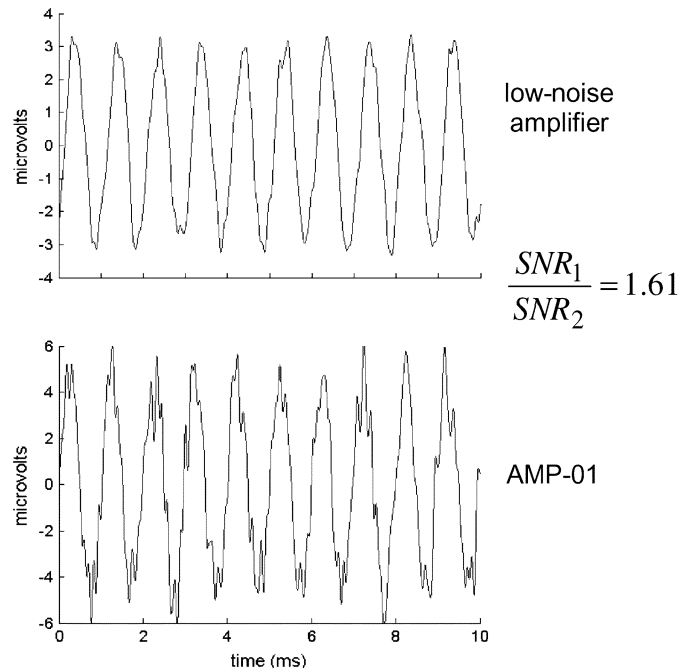


Fig. 8. Sample signals recorded with the proposed and AMP-01 amplifiers using the setup in Fig. 7. Ten cycles of the recorded signals are plotted to illustrate the difference in SNRs with each amplifier. Signals are FIR filtered between 500 Hz–10 kHz on the computer. SNR of the low-noise amplifier is 1.61 times larger than that of the AMP-01 amplifier. Notice that the signal amplitude is smaller with the low-noise amplifier, because the finite value of the amplifier’s input impedance (10 $\text{k}\Omega$) attenuates the source signal.

amplitude is set to a value in the microvolt range that is representative of peripheral nerve signals. The noisy signal was acquired into the computer at 200 ksamples/s, and the SNR was calculated as the root mean square (rms) value of the sinusoidal signal divided by the total noise voltage integrated from 500 Hz to 10 kHz. The SNR of the signal recorded with the low-noise amplifier is 1.61 times higher than that of AMP-01. Notice that the signal amplitude is smaller with the low-noise amplifier, because the magnetizing coil impedance (10 $\text{k}\Omega$) in series to the cuff attenuates the source signal. However, this does not affect the SNR since the thermal noise of the source (e_T) is reduced by the same factor.

VI. DISCUSSION AND CONCLUSION

The proposed circuit takes advantage of the noise-matching concept and the fact that FETs have a very low input current noise. The total input noise with this design is very close to the theoretical thermal noise level of the source impedance (Fig. 5), indicating that the electronic noise contribution ($\overline{e_n}$ and $\overline{i_n}$) to (3) is minimal. It is important to realize that there are secondary noise sources in the circuit that are not accounted for in the calculations. For instance, the flicker (or $1/f$) noise that junction field-effect transistors (JFETs) exhibit is not considered in the noise analysis, which, according to the manufacturer, decays quickly above 100 Hz and, thus, should become negligible within the frequency range of the neural signals. However, the elevation at the lower end of the spectrum in Fig. 5 is most likely due to the flicker noise that is present in the input current noise.

As a comparison, the input voltage and current noise for AMP-01 are given as 5 nV/ $\sqrt{\text{Hz}}$ and 0.15 pA/ $\sqrt{\text{Hz}}$ (10 Hz–10 kHz) by the manufacturer. The input voltage noise of 5 nV/ $\sqrt{\text{Hz}}$ alone is equivalent to the thermal noise of a 1520- Ω resistor at 20°C (5). The electronic noise contribution of this amplifier to sources smaller than a few times this resistor value would be significant. For instance, the total input noise (electronic + thermal) for $R_s = 1 \text{ k}\Omega$ at 20°C would theoretically be 6.4 nV/ $\sqrt{\text{Hz}}$ (3) whereas the source alone would have only 4 nV/ $\sqrt{\text{Hz}}$. The actual noise level measured with the AMP-01 amplifier built for this report varied between 6 and 7 nV/ $\sqrt{\text{Hz}}$ for $R_s = 1 \text{ k}\Omega$ (Fig. 6). AMP-01 is one of the best bipolar input amplifiers to be used with small source resistances ($R_{so} = 33 \text{ k}\Omega$), but its noise contribution is still significant for $R_s = 1 \text{ k}\Omega$. In the proposed design, despite the fact that the voltage noise of J201 (6 nV/ $\sqrt{\text{Hz}}$) is higher than that of AMP-01, it allows one to use a large turn-ratio transformer. The large turn-ratio implies that the input referred noise will be so many times (n) smaller.

Alternatively, if AMP-01 was noise matched to a 1.5-k Ω source with a transformer of $n = 5$ [using (2), $n = 4.7$], the total electronic noise

contribution at mid-frequencies would be 1.5 nV/ $\sqrt{\text{Hz}}$ (compare with 0.6 nV/ $\sqrt{\text{Hz}}$ for $n = 10$ and 0.1 nV/ $\sqrt{\text{Hz}}$ for $n = 82$ with the proposed design, see Fig. 3). Although this is a significant improvement, it is still not nearly as good as the current design.

The proposed design is near optimal and practical when all the design criteria, e.g., the bandwidth, turn ratio and the size of the transformer, the total noise, and the power consumption of the circuit are considered. Because the circuit needs only 97 μA for power, it may be feasible to incorporate this design into implantable devices that are powered transcutaneously. (As a reference point, AMP-01 requires 4.8 mA, as specified by the manufacturer.) The transformer PICO 24500 may be considered large for some applications ($D = 19 \text{ mm}$, $L = 18 \text{ mm}$). Smaller, surface-mount versions of these transformers (PICO, Series 7000, $7.9 \times 7.9 \times 8.2 \text{ mm}$) are commercially available.

REFERENCES

- [1] M. Sahin, D. M. Durand, and M. A. Haxhiu, "Chronic recordings of hypoglossal nerve in a dog model of upper airway obstruction," *J. Appl. Physiol.*, vol. 87, no. 6, pp. 2197–2206, 1999.
- [2] M. Sahin and D. M. Durand, "Signal-to-noise ratio of nerve signals recorded with full and open cylinder cuff electrodes," in *Proc. 21th Ann. Int. Conf. IEEE/EMBS*, 1999.
- [3] J. P. Fish, *Electronic Noise and Low Noise Design*. New York: McGraw-Hill, 1994, pp. 91–120.
- [4] J. G. Webster, *Medical Instrumentation: Application and Design*, 3rd ed. New York: Wiley, 1998, p. 113.
- [5] R. B. Stein, D. Charles, L. Davis, J. Jhamandas, A. Mannard, and T. R. Nichols, "Principles underlying new methods for chronic neural recording," *Can. J. Neurol. Sci.*, pp. 235–244, Aug. 1975.
- [6] Z. M. Nikolic, D. B. Popovic, R. B. Stein, and Z. Kenwell, "Instrumentation for ENG and EMG recordings in FES systems," *IEEE Trans. Biomed. Eng.*, vol. 41, no. 7, pp. 703–706, Jul. 1994.
- [7] M. Sahin and D. M. Durand, "An interface for nerve recording and stimulation with cuff electrodes," in *Proc. 19th Ann. Int. Conf. IEEE/EMBS*, vol. 5, Oct. 30–Nov. 2 1997.